Effects of US3 protein kinase activity on localization of UL31/UL34 protein and nucleocapsids egress of duck plague virus

Liyao Deng,[*,‡,§,1] Anchun Cheng,[*,‡,§,1] Mingshu Wang,[*,‡,§,2] Wei Zhang,[†] Bin Tian,[*,‡,§] Ying Wu,[*,‡,§] Qiao Yang,[*,‡,§] Xumin Ou,[*,‡,§] Sai Mao,[*,‡,§] Di Sun,[*,‡,§] Shaqiu Zhang,[*,‡,§] Juan Huang,[*,‡,§] Qun Gao,[*,‡,§] Xinxin Zhao,[*,‡,§] Renyong Jia,[*,‡,§] Shun Chen,[*,‡,§] Mafeng Liu,[*,‡,§] and Dekang Zhu[†,§]

[*]*Institute of Preventive Veterinary Medicine, Sichuan Agricultural University, Chengdu City, Sichuan, 611130, PR China;* [†]*Sinopharm Yangzhou VAC Biological Engineering CO., Ltd., Yangzhou City, Jingshu, 225100, PR China;* [‡]*Key Laboratory of Animal Disease and Human Health of Sichuan Province, Sichuan Agricultural University, Chengdu City, Sichuan, 611130, PR China; and* [§]*Avian Disease Research Center, College of Veterinary Medicine, Sichuan Agricultural University, Chengdu City, Sichuan, 611130, PR China*

ABSTRACT Duck plague virus (**DPV**) is a pathogen causing duck plague and has caused huge economic losses in poultry industry. In our previous report, US3 gene deletion from DPV genome seriously impaired virus replication. In this study, we constructed a US3 kinase-inactive mutant (**US3K213A**) to further explore the function of US3 protein (**pUS3**) in DPV. Our results showed that the loss of pUS3 kinase activity caused lower viral titers, smaller plaque sizes and a blockage of capsids nuclear egress including primary enveloped virion (**PEV**) accumulation compared to the parental virus infection. It indicates that the effects of DPV pUS3 on viral propagation depended on its kinase activity. In addition, we conducted electron microscopy analysis to show the outer nuclear membrane (**ONM**) evaginations and the nuclear envelope (**NE**) deep invagination in US3K213A-infected cells. Finally, an irregular distribution of pUL31/pUL34 in the NE in △US3- and US3K213A-infected cells and an interaction of pUS3 and pUL31 were found, which suggests that pUS3 potentially targets pUL31 and regulates the localization of pUL31/pUL34 to promote nucleocapsids egress through its kinase activity.

Key words: duck plague virus, US3, nucleocapsids egress, UL31/UL34

INTRODUCTION

Duck plague virus (**DPV**), also known as duck enteritis virus (**DEV**), induces an acute contagious viral disease with high morbidity and mortality in waterfowl, resulting in serious economic losses (Dhama et al., 2017). DPV belongs to a member of the subfamily of *Alphaherpesvirinae*, which includes herpes simplex virus (**HSV**), pseudorabies virus (**PRV**), bovine herpesvirus (**BHV**), and Marek's disease virus (**MDV**). The diameter of DPV is approximately 150 to 300 nm, and its structure consists of a capsid containing viral DNA, surrounded by tegument and a viral envelop (Yuan et al., 2005; Guo et al., 2009; Cheng, 2015).

US3 homologs encode Ser/Thr protein kinases and their consensus phosphorylation target sequence is $R_nX(S/T)YY$, where n is ≥ 2; X can be absent or any amino acid, but preferably Arg, Ala, Val, Pro, or Ser; S/T is the target site where either Ser or Thr is phosphorylated; and Y can be any amino acid except proline or an acidic residue (Deruelle and Favoreel, 2011). In HSV, US3 protein (**pUS3**) alone phosphorylates specific protein kinase A (**PKA**) substrates to block apoptosis, suggesting that its target site specificity is similar to that of PKA (Benetti and Roizman, 2004). Thus, anti-phospho-PKA substrate antibodies were sometimes used to detect US3 protein kinase activity (Kato et al., 2011). Moreover, US3 homologs contain a highly conserved ATP-binding domain and a catalytic domain in which the invariant residues are critical and are often targets for mutagenesis in construction of US3 kinase-inactive mutants (Deruelle and Favoreel, 2011).

Protein kinase activity is an inseparable part of pUS3 in its functions in other alphaherpesviruses. For

example, HSV pUS3 phosphorylates viral proteins glycoprotein B (gB) (Kato et al., 2009), UL31 (Mou et al., 2009), UL34 (Ryckman and Roller, 2004), and UL47 (Kato et al., 2011) to facilitate virion assembly and maturation. PRV pUS3-induced alterations in the host cytoskeleton enhance intercellular virus spread through its kinase activity (Favoreel et al., 2005; Van den Broeke et al., 2009). Whereas some US3 mutants with point mutations near or within the kinase catalytic domain have no effect on the cell cytoskeleton (Brzozowska et al., 2010). Moreover, HSV pUS3 hyperphosphorylates p65 and phosphorylates TRAF6 by its kinase activity to inhibit NF-κB activation and promote viral immune evasion (Deng et al., 2018).

In other herpesviruses, capsids nuclear egress is a complicated process that involves several viral proteins. Nuclear egress complex (**NEC**), a heterodimeric complex of pUL31 and pUL34, is indispensable for herpesvirus nuclear egress where UL34 as a type II membrane protein tethers NEC to the inner nuclear membrane (**INM**) and pUL31 is exposed to the nucleoplasm (Mettenleiter et al., 2013). In addition, pUL17 and pUL25 also participate in capsids nuclear egress. In this process, pUL25 is required for the association of pUL31 with capsids, and the interaction of pUL25 and pUL31 exposed in the nucleoplasm helps to select C capsids (mature capsids) for primary envelopment. Then pUL34 interacts with lamin A/C directly or indirectly to promote localization of pUL34 in the nuclear envelope (NE), also known as the nuclear membrane. Protein kinases, including pUS3, are recruited to thin nuclear lamina to phosphorylate and dissolve them, thereby facilitating capsids budding and nuclear egress (Mou et al., 2008; Johnson and Baines, 2011; Mettenleiter et al., 2013).

A lot of work on DPV has been completed in our laboratory, which means we have relatively mature and reliable methods to study DPV (Hu et al., 2017; You et al., 2018; He et al., 2020). Our previous report demonstrated that DPV US3 gene deletion significantly impaired viral replication (Deng et al., 2020). To further investigate the functions of pUS3 kinase activity in DPV replication, we constructed a recombinant virus US3K213A, where lysine at site 213 (**Lys-213**) of US3 sequence located within the catalytic domain was substituted by alanine. The recombinant virus was constructed based on an infectious bacterial artificial chromosome (**BAC**) containing the genome of DPV Chinese virulent strain (**CHv**), and US3K213A virus was identified as a US3 kinase-inactive mutant using western blot. Furthermore, plaque sizes, growth curves and viral morphogenesis of US3K213A virus were examined. Results revealed that the effects of pUS3 on viral titers, cell-to-cell spread and nucleocapsids egress all depended on its kinase activity in DPV. Cells infected with US3K213A virus also showed the outer nuclear membrane (**ONM**) evaginations and NE deep invagination. Finally, an aberrant distribution of NEC

proteins in the NE of △US3- and US3K213A-infected cells and an interaction of pUS3 and pUL31 were observed, suggesting that DPV nucleocapsids egress may be involved in localization of pUL31/pUL34 regulated by pUS3 kinase activity through the interaction of pUS3 and pUL31. Our results shed new light on further understanding of DPV pUS3 functions in viral replication.

MATERIALS AND METHODS

Cell, Viruses and Antibodies

Duck embryo fibroblast (**DEF**) cells were harvested from 9-day-old duck embryos and incubated in minimal essential medium (**MEM**, Gibco Life Technologies, Shanghai, China) containing 10% newborn bovine serum (**NBS**, Gibco, Grand Island, NY) at 37°C with 5% CO_2. The parental virus (**BAC-CHv**) with enhanced green fluorescent protein (**EGFP**) expression (Wu, 2015), also named wild-type (**WT**) virus in this study, and a recombinant virus BAC-CHv-US3-Flag (**US3-Flag**) were both obtained from our research center. Mouse anti-US3 polyclonal antibody was prepared in our laboratory. The phospho-PKA substrate (RRXS*/T*) (100G7E) rabbit monoclonal antibody was purchased from Cell Signaling Technology (CST, Danvers, MA). Mouse monoclonal anti-Flag and anti-HA antibodies were purchased from Medical & Biological Laboratories (MBL, Japan), and mouse anti-actin monoclonal antibody was purchased from TransGen Biotech (China).

Plasmid Construction

The DNA sequences of DPV US3, UL31, and UL34 were amplified from CHv strain genome and US3^{K213A} was obtained through overlap PCR. All of them were cloned into the pCAGGS expression vector with a tag at the C terminus, named pCAGGS-UL31-HA, pCAGGS-UL34-Flag and pCAGGS-US3^{K213A}-His. All primers used in this study are listed in Table 1.

Construction of Recombinant Virus US3K213A

Briefly, a fragment of US3K213A was amplified from pCAGGS-US3^{K213A}-His, and then the DNA fragment in which the US3^{K213A} sequence, an I-SceI site, a KanR cassette and a 40-bp sequence duplication were flanked by 40-bp homology arms was obtained through overlap PCR. Then, the DNA fragment was electroporated into GS1783 containing pBAC-CHv-△US3 to induce the first Red recombination through the 40-bp flanking homology arms, resulting in the insertion of US3^{K213A} sequence and KanR cassette. Subsequently, the induction of I-SceI expression by L-arabinose and resulting cleavage of the I-SceI site generated new substrates for the second Red recombination, and then new substrates

Table 1. All primers in this study.

Primer name	Sequence 5′-3′	Product
UL31-HA-F	catcattttggcaaagaattcGCCACCATGGCCATGTCTGACTACGATACCACAA	
UL31-HA-R	ttggcagagggaaaaagatctTTAAGCGTAATCTGGAACATCGTATGGGTAGCGAGGAGGAGGAAAATCGT	UL31-HA
UL34-Flag-F	catcattttggcaaagaattcGCCACCATGGAACAGCTTTACCCATGT	
UL34-Flag-R	ttggcagagggaaaaagatctTTACTTATCGTCGTCATCCTTGTAATCGATACGGCCACCAAAAGGC	UL34-Flag
US3-His-F	catcattttggcaaagaattcGCCACCATGGAAACGTGTCATACCGAT	
US3-His-R	ttggcagagggaaaaagatctTTAATGATGATGATGATGATGCCCTTTGTGGGTAATAAC	US3^{K213A}-His
mutUS3-F	ATACACCGCGACGTAGCACTTGAAAATAT	
mutUS3-R	GCTACGTCGCGGTGTATTATTCCTCTTC	
RUS3-F	GATTGCTCATATCAAACGAGAACAAACATACAAAACTGCCGCGGACGCAGCTCAAATGAAATGGAAACGTGTCATACCGAT	US3/US3^{K213A}
RUS3-R	ACTCCTCCCATATATTAATTGTAATTTACCCTTTGTGGGTAATAAC	
RUS3-Kan-F	ATTACAATTAATATATGGGAGGAGTCAAGTTTGTAAAAAAGTGTATAAATTAGGGATAACAGGGTAATCGAT	KanR
RUS3-Kan-R	ATCGCCGCAACGCGCATAGCTACTTGTCTAATTTATACACTTTTTTACAAACTTGACTCCTCCCATATATTAATTGTAATTGTTACAACCAATTAACC	

were integrated through the 40-bp sequence duplication, resulting in removal of the KanR cassette. Finally, constructed pBAC-CHv-US3^{K213A} plasmid was extracted and sequenced, and the confirmed plasmid was transfected into DEF cells according to the introduction of Lipofectamine 3000 transfection reagent (Thermo-Fisher, Carlsbad, CA) to produce US3K213A virus. Construction of the revertant virus (**RUS3**) was similar to that of US3K213A, and the only difference was that the DNA fragment has US3 sequence, not US3^{K213A} (Deng et al., 2020). Primers used in this study are shown in Table 1. The rescued viruses were identified by western blot.

Western Blot Analysis

An anti-phospho-PKA rabbit monoclonal antibody was used to detect DPV US3 protein kinase activity through detecting phosphorylated substrates of pUS3 (Kato et al., 2009; Kato et al., 2011). Briefly, DEF cells in 6-well plates were infected with 0.05 multiplicity of infection (**MOI**) of WT, US3K213A, △US3 and the revertant virus. At 48 h postinfection (**hpi**), protein lysates were collected in RIPA buffer with PMSF and phosphatase inhibitor added in advance. All samples were analyzed by western blot and detailed steps of western blot have been described in our previous study (He et al., 2020). Protein phosphorylation was detected by anti-phospho-PKA antibody, mouse anti-US3 polyclonal antibody was used to analyze pUS3 expression, rabbit anti-UL47 polyclonal antibody was used to detect pUL47 as an internal viral control, and actin protein was as a control for total proteins in cells.

Plaque Morphology

DEF cells in 6-well plates were infected with 0.001 MOI of US3K213A, △US3, WT virus and the revertant virus. After 2 h incubation at 37°C with 5% CO_2, the cells were washed and 1% methylcellulose (Solarbio, Beijing, China) was added. At 72 hpi, fluorescent plaques were observed and photographed under a microscope

(Nikon TI-SR, Japan), and the average plaque sizes were measured and analyzed.

Viral Growth Curves

DEF cells in 24-well plates were infected with 0.05 MOI of US3K213A, △US3, WT virus and the revertant virus. Intracellular and supernatant viruses were harvested at 24, 48, and 72 hpi, respectively, and then viral titers of all samples were detected using 50% tissue culture infectious dose (**TCID$_{50}$**) on DEF cells. All experiments were repeated 3 times.

Indirect Immunofluorescence Assay

At 6 h post transfection of pCAGGS-UL31-HA or pCAGGS-UL34-Flag, DEF cells were infected with 0.01 MOI of US3K213A, △US3, and WT virus. At 42 hpi, the cells were washed with phosphate-buffered saline (**PBS**) and fixed with 4% paraformaldehyde overnight at 4°C. Then, the cells were washed with PBS containing 0.1% Tween 20 (**PBST**) three times, permeabilized with 0.25% Triton X-100 for 30 min at 4°C, and incubated with 5% BSA for 1 h at 37°C. The cells were washed with PBST three times and incubated with mouse anti-HA/Flag tag antibody overnight at 4°C, washed three times with PBST, and subsequently incubated with Alexa-568 goat anti-mouse IgG (Thermo Fisher) for 45 min at 37°C. Finally, the cells were washed with PBST, incubated with DAPI for 5 min at room temperature, and washed again. The coverslips were sealed with glycerine buffer and photographed under a fluorescence microscope (Nikon ECLIPSE 80i, Japan).

Electron Microscopy Analysis

DEF cells in 6-well plates were infected with 5 MOI of US3K213A, △US3 and WT virus. At 20 hpi, the cells were scraped and collected in eppendorf tubes, centrifuged to pellet cells, and fixed with fresh 2.5% glutaraldehyde at 4°C for 2 h. Samples were sent to the Harbin Veterinary Research Institute (Harbin, China) for

analysis under a transmission electron microscope (Hitachi H-7650, Tokyo, Japan).

Coimmunoprecipitation (Co-IP) Assay

Transfected HEK 293T cells in 6-well plates with plasmids expressing pUS3 and pUL31 were lysed in IP lysis buffer (1% Triton X-100 and 0.5% sodium deoxycholate were dissolved in PBS) and incubated on ice for 30 min. The lysates were transferred to eppendorf tubes and centrifuged for 10 min at 4°C, and the supernatant was collected and added anti-HA/Flag antibody. The samples were incubated on a circular tube rotator overnight at 4°C, and then Protein A+G agarose (Beyotime, China) was added for 3 h incubation at 4°C again. The agarose was centrifuged and washed 3 times with IP lysis buffer at 4°C. Finally, the agarose was resuspended in 50 μL protein loading buffer, heated for 10 min, and centrifuged to harvest supernatant to perform western blot assay.

Mass Spectrometry

DEF cells in 10 cm dishes were infected with 0.05 MOI of recombinant virus US3-Flag. At 48 hpi, cells were lysed to harvest protein samples for IP assay using anti-Flag antibody. Finally, the immunoprecipitated samples were sent to PTM Biolabs (Hangzhou, China) for liquid chromatography-tandem mass spectrometry (**LC-MS/MS**) analysis.

Statistical analysis

The comparisons between the different groups were made by t tests with GraphPad Prism 6 software. The data was presented as the mean $\pm$ standard deviation (**SD**). P value (*P) <0.05 was considered significantly difference.

RESULTS

### Construction of A DPV US3 Kinase-inactive Mutant

In our previous report, we described the effects of pUS3 on DPV replication through a DPV US3-deleted mutant, and found that DPV pUS3 promoted virus cell-to-cell spread and virion nuclear egress (Deng et al., 2020). To further investigate the role of the kinase activity of pUS3 in DPV replication, we aligned the predicted catalytic domain of DPV US3, comprising residues 207 to 218, with its homologs in other alphaherpesviruses (Figure 1A), and chose Lys at site 213 as a target due to its high conservation and its demonstrated importance in MDV pUS3 kinase activity (Schumacher et al., 2008). We constructed a DPV US3K213A mutant where the Lys-213 was substituted by Ala based on BAC system as described in the materials and methods, and then conducted western blot assays to test pUS3^{K213A} kinase activity by using an anti-phospho-PKA antibody, which has been reported for detecting phosphorylated substrates of pUS3 in other alphaherpesviruses (Kato et al., 2009; Kato et al., 2011). As shown in Figure 1B, some significant phosphorylated bands were detected by the anti-phospho-PKA antibody in WT- and the revertant virus-infected cells, while the corresponding bands disappeared in △US3- or US3K213A-infected cells. It indicates that the anti-phospho-PKA antibody was able to detect phosphorylated substrates of DPV pUS3 and there was no pUS3 kinase activity in US3K213A- and △US3-infected cells. In addition, pUS3 was only expressed in US3K213A-, WT- and the revertant virus-infected cells but not in △US3-infected cells as expected, and pUL47 was expressed in all groups.

Growth Characteristics of US3K213A Mutant

To examine the effects of pUS3 kinase activity on viral growth properties, plaque morphology of US3K213A
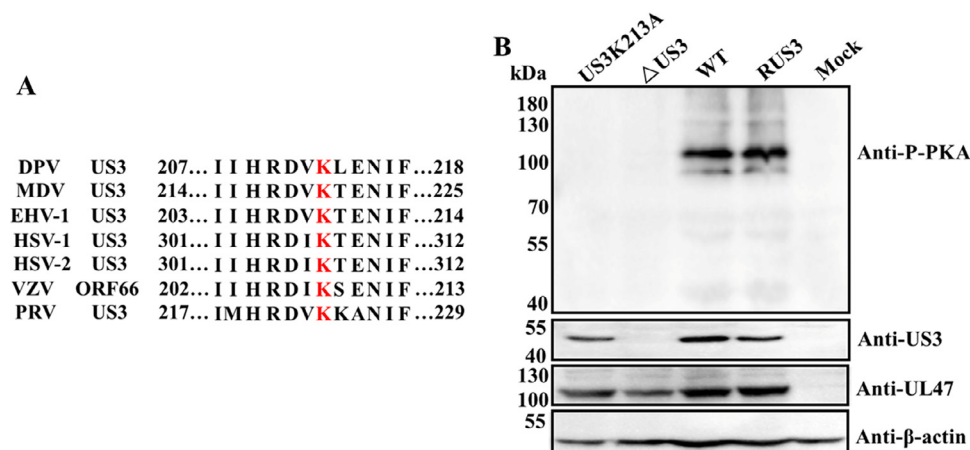
Figure 1. Construction of DPV US3K213A virus. (**A**) Amino acid sequence alignment of catalytic domains of DPV US3 protein and its homologs in other alphaherpesviruses. Lys-213 that was altered in this study is shown in red marker. (**B**) Identification of pUS3 kinase activity in US3K213A-infected cells. DEF cells were infected with US3K213A, △US3, WT and revertant virus. At 48 hpi, protein lysates were collected in RIPA buffer and western blot analysis was performed. Protein phosphorylation was detected using anti-phospho-PKA antibody. Expression of pUS3, pUL47 and actin was also tested using the corresponding antibodies. pUL47 was used as a control for viral proteins and actin was used as a control for whole proteins in host cells.
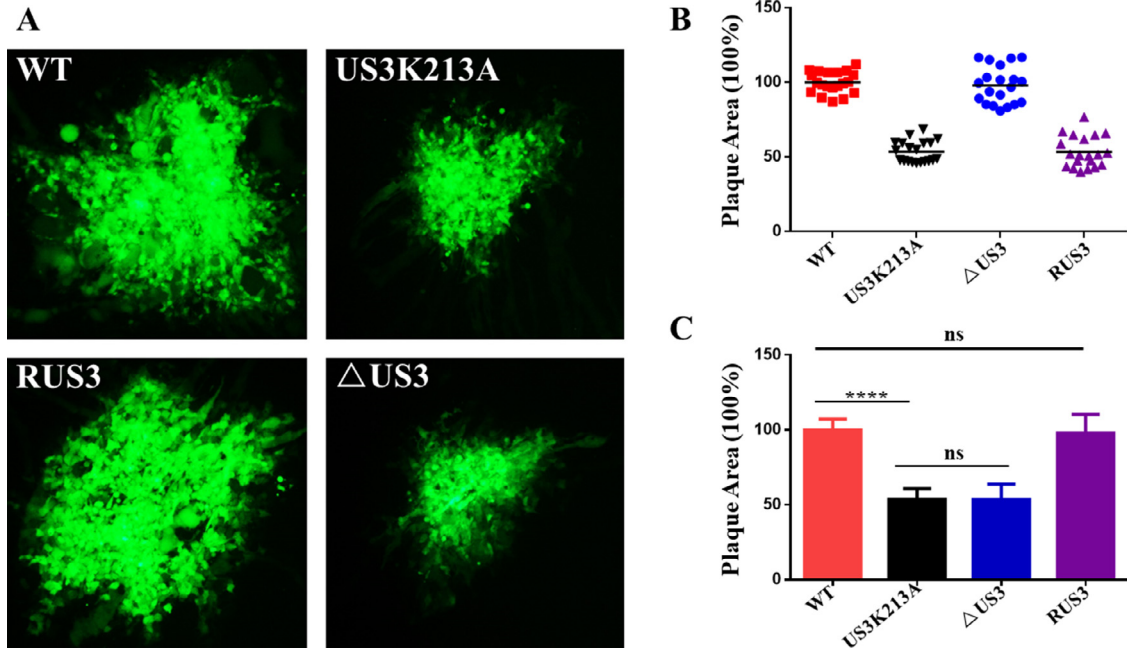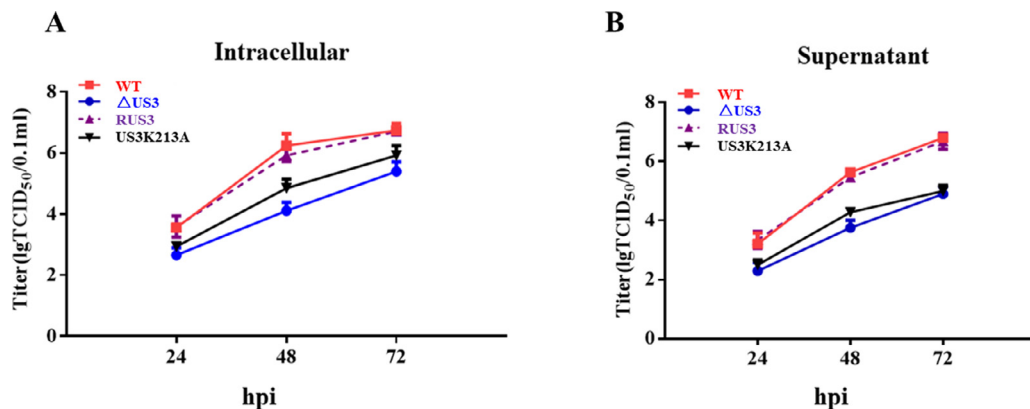
Figure 2. Plaque morphologies. (A) Green fluorescent plaques of US3K213A, △US3, WT and the revertant virus. DEF cells were infected with 0.001 MOI of US3K213A, △US3, WT and the revertant virus. After 2 h incubation with virus, the cells were washed and added 1% methylcellulose. At 72 hpi, the cells were fixed and fluorescent plaques were photographed. (**B**) and (**C**) Statistical analysis of twenty randomly selected viral green fluorescent plaques of US3K213A, △US3, WT and the revertant virus. Error bar represents the standard error of the mean. ****$P < 0.0001$.

mutant was monitored at 72 hpi. We already reported that DPV △US3-infected cells showed significantly reduced plaque sizes (Deng et al., 2020). Similarly, the plaque sizes of US3K213A were also observably smaller than those of WT virus and the revertant virus (Figure 2A). Moreover, 20 randomly selected plaques generated by US3K213A, △US3, WT or the revertant virus were statistically analyzed. As shown in Figure 2B and C, the plaque sizes of US3K213A were significantly smaller than those of WT virus ($P < 0.0001$), but there was no significant difference in plaque sizes between US3K213A and △US3. Therefore, the results suggested that the lack of pUS3 kinase activity impaired viral cell-to-cell spread.

Simultaneously, viral growth curves of these strains were also investigated. As shown in Figure 3, the growth efficiency of WT virus and the revertant virus

was at a similar level regardless of the intracellular source or supernatant source. However, viral titers of US3K213A from intracellular source were significantly lower than those of WT virus, with an approximately 25-fold reduction at 48 hpi and 7-fold at 72 hpi (Figure 3A). In Figure 3B, viral titers of US3K213A from supernatant source decreased nearly 20-fold at 48 hpi and 63-fold at 72 hpi compared to those of WT virus, with greater difference in supernatant compared to intracellular source at 72 hpi, indicating that the lack of pUS3 kinase activity might inhibit the release of infectious virions to supernatant. In addition, the growth curve of US3K213A had a slightly higher rate than that of △US3, suggesting that other domains besides the catalytic domain of pUS3 were functional in DPV replication.

Figure 3. Viral growth curves. DEF cells were infected with 0.05 MOI of US3K213A, △US3, WT and the revertant virus, and intracellular (**A**) and supernatant (**B**) viral titers were measured for the $TCID_{50}$ at 24, 48, and 72 hpi. All experiments were repeated three times.
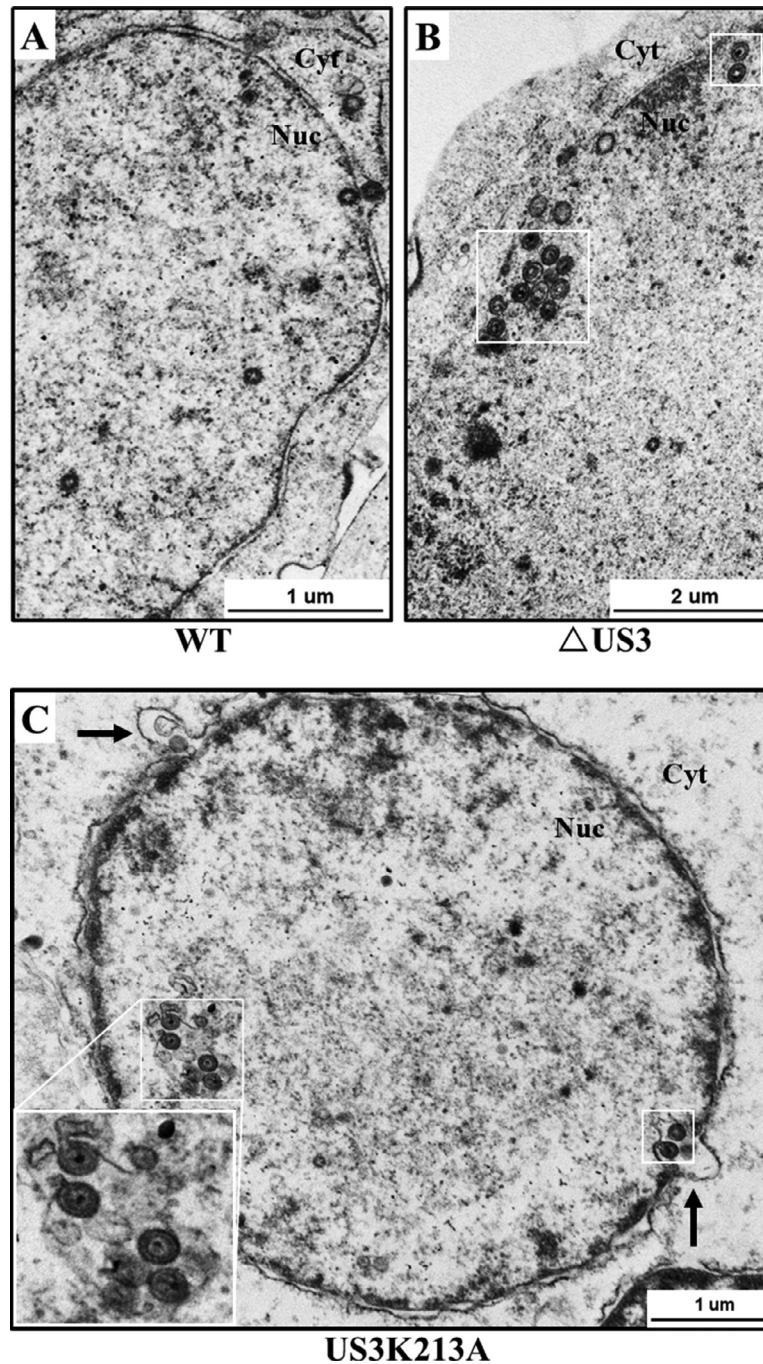
Figure 4. Accumulation of PEVs in WT-, △US3-, and US3K213A-infected cells. DEF cells infected with 5 MOI of WT, △US3, and US3K213A were fixed at 20 hpi, and analyzed by electron microscopy. White boxes indicate PEVs accumulation and black arrows indicate the ONM evaginations. (**A**) WT virus. (**B**) △US3 mutant. (**C**) US3K213A mutant.

Accumulation of PEVs in US3K213A-infected Cells

To investigate the role of pUS3 kinase activity in virion nuclear egress, US3K213A-infected cells were analyzed using electron microscopy. As shown in Figure 4A, in WT virus-infected cells, the nuclear membranes showed a smooth appearance with occasional perturbation by an egressing capsid, and no PEV accumulation was observed. In contrast, US3-deleted mutant caused an accumulation of PEVs trapping in the nucleus (Figure 4B, white boxed areas), indicating that pUS3 was functional in capsids nuclear egress, which is

consistent with our previous work (Deng et al., 2020). In Figure 4C, we also observed PEVs accumulation in US3K213A-infected cell (white boxed areas), implying that the kinase activity was necessary for pUS3-regulated nucleocapsids egress. To further confirm, a quantitative analysis of virions at different morphogenetic stages between WT virus and US3K213A virus was performed based on 19 infected cells. As presented in Table 2, cells infected with WT virus showed that 39% of virions were found in the nucleus and only 0.9% were seen in the perinuclear space (**PNS**), with most virions (60.1%) observed in the cytoplasm and extracellular space. However, in US3K213A-infected cells, 59.8% of

Table 2. Virions observed in WT or US3K213A virus-infected DEF cells.

| | % of virions in morphogenetic stage (of virions in stage) | | | |
| | Nucleus | | | |
Virus	Intranuclear	PNS	Cytoplasm and extracellular	Total counted (virions/cells)
DPV WT	39% (278)	0.9% (6)	60.1% (429)	713/19
DPV US3K213A	59.8% (367)	4.4% (27)	35.8% (220)	614/19

virions were found in the nucleus, around 1.5-fold higher than those of WT virus, and 35.8% were in the cytoplasm and extracellular space, approximately 1.7-fold decrease compared to WT virus. Particularly, there were 4.4% of virions observed in the PNS in US3K213A-infected cells, almost 5-fold increase compared to those of WT virus, further indicating that capsids nuclear egress regulated by pUS3 relied on its kinase activity. Additionally, it is worth noting that big, localized perturbations caused by evaginations of the ONM were also observed in US3K213A-infected cells (Figure 4C, black arrows), which were rarely found in WT virus-infected cells. Interestingly, Gao et al. put forward a new viewpoint about HSV pUS3 function in capsids nuclear egress that the lack of pUS3 was the cause of the INM herniation rather than PEVs accumulation (Gao et al., 2020). Therefore, it might explain our results that the absence of pUS3 kinase activity possibly caused evaginations of the ONM.

NE Deep Invagination in US3K213A-infected Cells

From our electron microscopy results, NE deep invagination was observed in US3K213A-infected cells, another phenotype that was noted. As shown in Figure 5A, the NE was only disturbed slightly in a small area in WT-infected cell. However, the nuclear morphology in US3K213A-infected cells had dramatic alterations with NE deep invagination in multiple areas (Figure 5B, black arrowheads). To further identify, a quantification analysis of cells with NE deep invagination was performed. Shown in Figure 5C, 21.4% of cells (28 cells in total) infected with WT virus showed NE deep invagination, whereas 51.9% of cells infected with US3K213A mutant (27 cells in total) were observed with NE deep invagination, almost 2.5-fold increase. Therefore, these results revealed that the lack of DPV pUS3 kinase activity might cause NE deep invagination in infected cells.
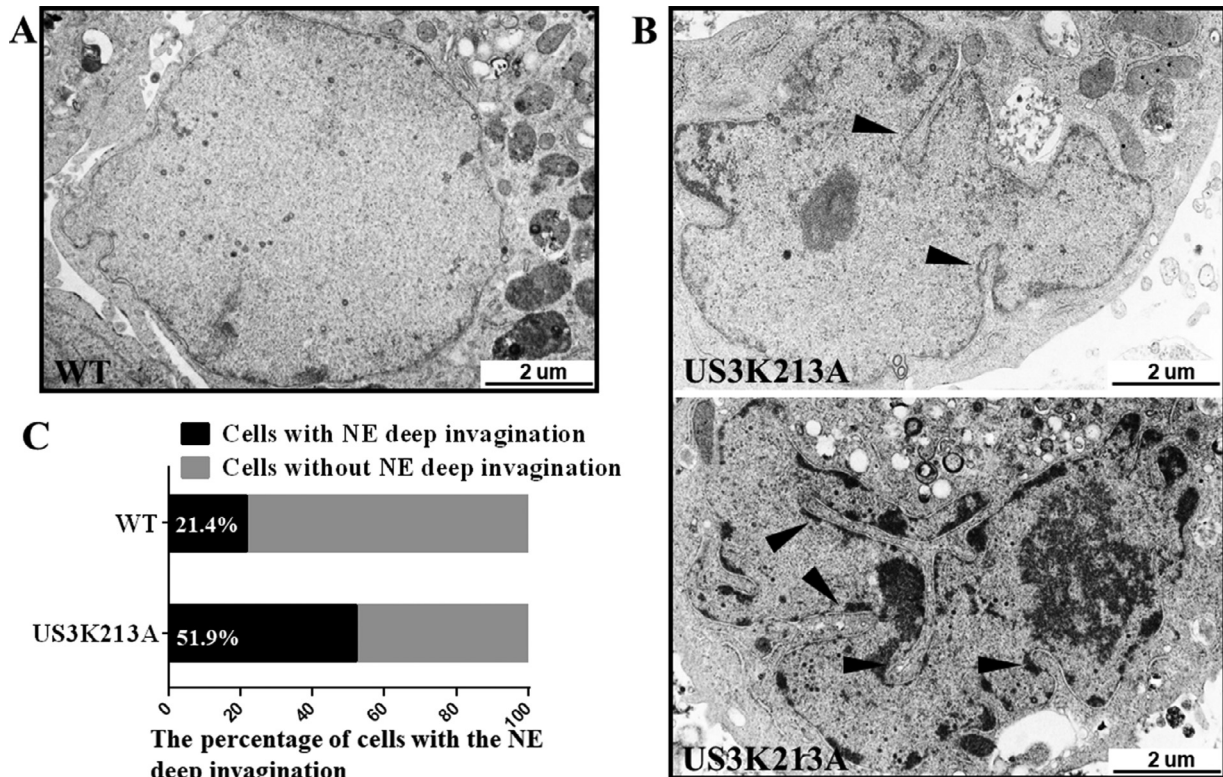
Figure 5. NE deep invagination in US3K213A-infected cells. DEF cells infected with 5 MOI of WT and US3K213A were fixed at 20 hpi, and analyzed by electron microscopy. (**A**) WT virus. (**B**) US3K213A virus. Black arrowheads indicate NE deep invagination. (**C**) Percentage of cells with NE deep invagination.

Table 3. MS analysis of the enrichment of pUS3.

Protein names	Gene names	MW [kDa]	Protein score	Sequence coverage (%)	# Unique peptides	# PSMs
Tegument protein VP22	UL49	27.85	290.20	44.66	8	13
Protein kinase	US3	42.94	276.40	24.16	9	15
Tegument protein UL47	UL47	87.92	242.13	17.77	12	12
US10	US10	36.01	208.48	16.46	4	5
Tegument protein UL37	UL37	118.22	149.35	6.10	6	6
LORF-3	LORF3	53.87	148.43	12.29	5	6
LORF4	LORF9	36.01	144.32	15.53	6	6
Alkaline nuclease	UL12	63.63	100.77	11.92	5	5
Nuclear egress protein 1	UL31	35.74	93.73	6.13	2	2
Multifunctional expression regulator	UL54	51.72	91.27	7.21	3	3
LORF5	LORF5	27.45	77.49	10.00	3	3
Nuclear egress protein 2	UL34	31.02	68.62	17.39	5	5
Envelope glycoprotein B	UL27	113.84	46.89	3.90	3	3
Cytoplasmic envelopment protein 1	UL7	36.00	32.51	3.74	1	1

Note: Nuclear egress proteins UL31 and UL34 were bolded.

Effects of pUS3 Kinase Activity on The Localization of pUL31 and pUL34

A mass spectrometry (**MS**) assay was carried out to identify potential proteins that might interact with pUS3. Some data are presented in Table 3. Several viral proteins were detected in the enrichment of DPV pUS3, including UL49, UL47, US10, UL37, LORF3, LORF4, UL12, UL31, UL54, LORF5, UL34, gB, and UL7. Due to the indispensable role of pUL31 and pUL34 in herpesvirus nuclear egress involving in their proper localization (Reynolds et al., 2001; Ryckman and Roller, 2004; Mou et al., 2009; Mettenleiter et al., 2013), we focused on proteins UL31 and UL34 and investigated their subcellular localization in WT-, △US3- and US3K213A-infected cells by fluorescence microscopy assays. There were no anti-UL31 and anti-UL34 antibodies in our lab, therefore, the plasmid expressing fusion protein UL31-HA or UL34-Flag was used. These fusion protein expression plasmids were transfected into DEF cells first, and then the DEF cells were further infected with WT, △US3 and US3K213A viruses at 6 h post-transfection. Representative images are shown in Figure 6A. Compared to WT virus-infected cells where pUL3l and pUL34 exhibited a smooth pattern throughout the NE, cells infected with △US3 virus and US3K213A mutant were observed with more punctate aggregates of pUL31 and pUL34 in the NE. We randomly selected 10 fields of view and counted the cells with punctate aggregates of pUL31 and pUL34. As shown in Figure 6B, 17.2% of WT-infected cells were observed with punctate localization of pUL31 in the NE. In comparison, 59.1% and 52.8% of cells infected with △US3 and US3K213A were seen with punctate localization respectively, almost three-fold increase from WT. Similarly, 4.4% cells infected with WT had punctate aggregates of pUL34 in the NE, whereas it was observed in 66.7% of △US3- and 81.7% of US3K213A- infected cells, at least 15-fold increase compared to WT. Therefore, these results indicated that the lack of pUS3 kinase activity caused an aberrant distribution of pUL31 and pUL34 in the NE with punctate aggregates, suggesting an essential role of DPV pUS3 kinase activity in proper localization of pUL31 and pUL34.
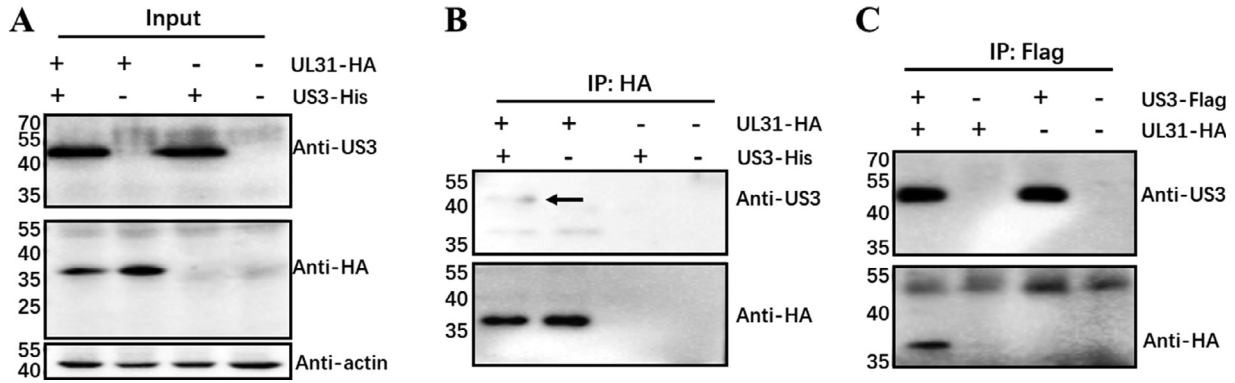
The interaction of pUS3 and pUL31

It was reported that HSV pUL31 is the major substrate of pUS3 kinase responsible for regulating the localization of pUL31/pUL34 at the nuclear rim (Mou et al., 2009). Therefore, interaction of DPV pUS3 and pUL31 was detected by Co-IP assay. As shown in Figure 7A, both pUS3 and pUL31 were expressed normally in the transfected cells. pUS3 was found in the enrichment of pUL31 (Figure 7B, black arrow), and pUL31 was also observed in the enrichment of pUS3 in a
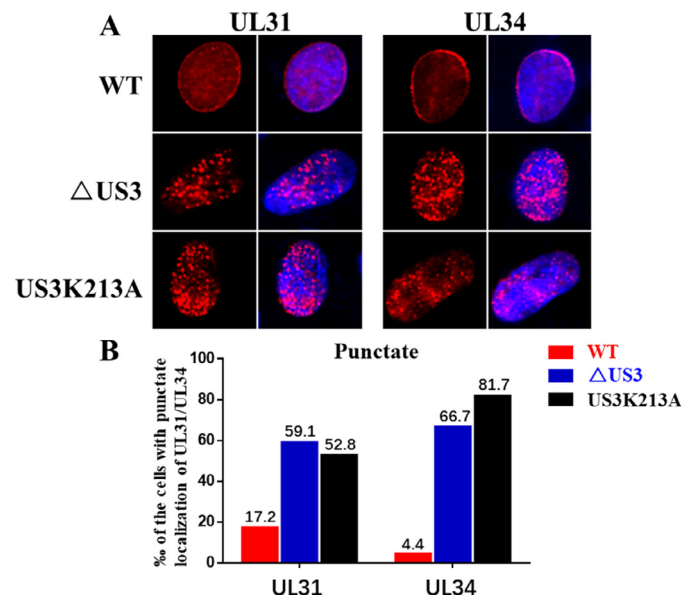
Figure 6. Localization of pUL31 and pUL34 in infected cells. DEF cells were transfected with the plasmid expressing fusion protein UL31-HA or UL34-Flag, and then infected with US3K213A, △US3 and WT at 6 h post-transfection. At 42 hpi, the cells were fixed to perform immunofluorescence assays. (**A**) Representative images of localization of pUL31 and pUL34 in WT-, △US3-, or US3K213A-infected cells. (**B**) Proportion of cells with punctate distribution of pUL31 and pUL34 in the NE.

Figure 7. Interaction between pUS3 and pUL31. HEK 293T cells were transfected with plasmids expressing pUS3 and pUL31. At 48 h post-transfection, the cells were lysed and protein samples were harvested to perform Co-IP and western blot. (**A**) Expression of pUS3 and pUL31 in transfected cells. (**B**) Detection of pUS3 in the enrichment of pUL31. Black arrow indicates the band of pUS3. (**C**) Detection of pUL31 in the enrichment of pUS3.

reciprocal experiment (Figure 7C), indicating that DPV pUS3 interacted with pUL31 directly. In addition, we didn't detect phosphorylation of pUL31 caused by pUS3 kinase activity using the anti-phospho-PKA antibody (data not shown). It is possible that the anti-phospho-PKA antibody couldn't react with pUL31 because of its substrate specificity. All data suggest that maybe pUS3 regulates the localization of pUL31/pUL34 to promote nucleocapsids egress through targeting pUL31.

DISCUSSION

In this study, to investigate the roles of pUS3 kinase activity in DPV replication, we constructed a US3 kinase-inactive mutant (US3K213A) where Lys at site 213 of pUS3 was substituted with Ala, and then assessed the mutant's biological characteristics. Our data suggest that the effects of pUS3 on DPV replication are connected to its kinase activity, including viral titers, cell-to-cell spread and capsids nuclear egress (Figures 2−4). However, US3K213A mutant had a slightly higher growth curve than that of △US3 (Figure 3), indicating that there might be other domains, such as autophosphorylation areas, in pUS3 that also play a role in DPV replication. In addition, a decrease of pUL47 expression was observed in △US3 or US3K213A-infected cells (Figure 1B), which was also found in our recently published report where it interpreted that DPV pUS3 phosphorylated pUL47 resulting in a possibility of increased stability of pUL47 in the cytoplasm (Deng et al., 2022).

Electron microscopy analysis (Figure 4) showed PEVs accumulation and the ONM evaginations in US3K213A-infected cell. It has been widely hypothesized that PEVs accumulation caused by herpesvirus US3-related mutants is a consequence of the failure of capsids de-envelopment at the ONM (Reynolds et al., 2002; Schumacher et al., 2008; Wisner et al., 2009; Proft et al., 2016), which involves pUS3-related gB phosphorylation (Wisner et al., 2009; Johnson and Baines, 2011). However, Gao et al recently proposed a new theory that the lack of pUS3 causes INM herniation rather than PEVs accumulation, and the INM herniation is independent of

PEVs accumulation because they were still formed in △UL16/△US3-infected cells where no PEVs were generated (Gao et al., 2020). Therefore, in addition to gB-regulated de-envelopment at the ONM, it is possible that PEVs accumulation observed in DPV US3K213A- or △US3-infected cells was caused by the ONM evaginations. Moreover, in a PRV study, PEVs accumulation was also observed when a significant enlarged PNS was generated by overexpression of a dominant negative SUN2 protein (Klupp et al., 2017), which might further explain that PEVs accumulation observed in our results was due to enlarged PNS caused by the ONM evagination.

In addition, Figure 5 showed that more cells with NE deep invagination were observed in US3K213A infection, compared to WT virus, with around 2.5-fold increase (Figure 5C). The NE with aberrant folding in US3K213A-infected cells resembled type II nucleoplasmic reticulum (**NR**), which involves in the whole NE invagination including the INM, the ONM and a diffusion-accessible cytoplasmic core (Malhas et al., 2011). However, the correlation between pUS3 and type II NR has never been reported so far. Perhaps the NE deep invagination in US3K213A-infected cells was apoptosis-induced nuclear morphological changes. It has been reported that pUS3 is a viral anti-apoptotic protein in herpesvirus, and it blocks apoptosis by phosphorylating procaspase-3, Bad, NF-κB, AKT, and PAKs which are all related to apoptosis pathways (You et al., 2017). Therefore, the lack of pUS3 kinase activity might promote apoptosis, resulting in the nuclear morphological changes in US3K213A-infected cells.

NEC containing viral pUL31 and pUL34 is sufficient for herpesvirus nuclear egress. In this process, proper localization of NEC with smooth and uniform distribution in the NE is important, because the discrete and round foci distribution of NEC has been shown to restrict potential envelopment sites (Mou et al., 2007). In our results, DPV nuclear egress was impaired by the lack of pUS3 kinase activity with capsids trapping in the nucleoplasm and PNS in the US3K213A-infected cells (Table 2). Moreover, pUL31 and pUL34 were detected

in the enrichment of pUS3 according to MS analysis (Table 3). Therefore, we investigated the localization of pUL31 and pUL34 in the absence of pUS3 kinase activity. Figure 6 showed that the localization of pUL31 and pUL34 was observed in an aberrant punctate distribution in △US3- and US3K213A-infected cells. Figure 7 showed an interaction of pUS3 and pUL31. They suggested that maybe the localization of pUL31/pUL34 was regulated by pUS3 kinase activity to promote nucleocapsids egress through the interaction of pUS3 and pUL31.

Interestingly, there were many viral proteins observed in our MS analysis (Table 3). In addition to UL47 (Kato et al., 2011), UL12 (Daikoku et al., 1995), UL31 (Mou et al., 2009), UL34 (Ryckman and Roller, 2004), gB (Kato et al., 2009), and UL7 (Shibazaki et al., 2020) which had been found to be phosphorylated substrates of pUS3 in other alphaherpesviruses, other proteins including UL49, US10, UL37, UL54, LORF3, LORF4, and LORF5 have still not been reported to interact with pUS3. Among these proteins, LORF3, LORF4 and LORF5 are unique genes in avian herpesviruses. Therefore, this result is really useful to explore different functions of DPV pUS3. In addition, it's surprising that there was no UL13 protein detected in the enrichment of pUS3. In HSV, pUL13 phosphorylated pUS3 and regulated the localization of NEC, but pUL13-mediated phosphorylation of pUS3 was not required for optimal pUS3 kinase activity (Kato et al., 2006). Maybe the function of pUL13-mediated phosphorylation of pUS3 is not conserved in herpesvirus, therefore, the interaction of pUS3 and pUL13 was not found in our results.

Overall, we investigated the effects of pUS3 kinase activity on DPV replication in this study, and found DPV viral titers, cell-to-cell spread, and capsids nuclear egress were regulated by pUS3 kinase activity, which might be involved in proper localization of NEC in the NE through the interaction of pUS3 and pUL31.

ACKNOWLEDGMENTS

DISCLOSURES

REFERENCES

Benetti, L., and B. Roizman. 2004. Herpes simplex virus protein kinase US3 activates and functionally overlaps protein kinase A to block apoptosis. Proc. Natl. Acad. Sci. 101:9411–9416.

Brzozowska, A., M. Rychłowski, A. D. Lipińska, and K. Bieńkowska-Szewczyk. 2010. Point mutations in BHV-1 Us3 gene abolish its ability to induce cytoskeletal changes in various cell types. Vet. Microbiol. 143:8–13.

Cheng, A. 2015. Duck Plague. China Agriculture Press, Beijing.

Daikoku, T., Y. Yamashita, T. Tsurumi, and Y. Nishiyama. 1995. The US3 protein kinase of herpes simplex virus type 2 is associated with phosphorylation of the UL12 alkaline nuclease in vitro. Arch. Virol. 140:1637–1644.

Deng, L., J. Wan, A. Cheng, M. Wang, B. Tian, Y. Wu, Q. Yang, X. Ou, S. Mao, D. Sun, S. Zhang, D. Zhu, R. Jia, S. Chen, M. Liu, X. Zhao, J. Huang, Q. Gao, Y. Yu, L. Zhang, and L. Pan. 2022. Duck plague virus US3 protein kinase phosphorylates UL47 and regulates the subcellular localization of UL47. Front. Microbiol. 13:876820.

Deng, L., M. Wang, A. Cheng, Q. Yang, Y. Wu, R. Jia, S. Chen, D. Zhu, M. Liu, and X. Zhao. 2020. The pivotal roles of US3 protein in cell-to-cell spread and virion nuclear egress of duck plague virus. Sci. Rep. 10:1–11.

Deng, L., Q. Zeng, M. Wang, A. Cheng, R. Jia, S. Chen, D. Zhu, M. Liu, Q. Yang, and Y. Wu. 2018. Suppression of NF-κB activity: a viral immune evasion mechanism. Viruses 10:409.

Deruelle, M., and H. Favoreel. 2011. Keep it in the subfamily: the conserved alphaherpesvirus US3 protein kinase. J. Gen. Virol. 92:18–30.

Dhama, K., N. Kumar, M. Saminathan, R. Tiwari, K. Karthik, M. A. Kumar, M. Palanivelu, M. Z. Shabbir, Y. S. Malik, and R. K. Singh. 2017. Duck virus enteritis (duck plague)−a comprehensive update. Vet. Q. 37:57–80.

Favoreel, H. W., G. Van Minnebruggen, D. Adriaensen, and H. J. Nauwynck. 2005. Cytoskeletal rearrangements and cell extensions induced by the US3 kinase of an alphaherpesvirus are associated with enhanced spread. Proc. Natl. Acad. Sci. 102:8990–8995.

Gao, J., R. L. Finnen, M. R. Sherry, V. Le Sage, and B. W. Banfield. 2020. Differentiating the roles of UL16, UL21, and Us3 in the nuclear egress of herpes simplex virus capsids. J. Virol. 94:e00738 -00720.

Guo, Y., A. Cheng, M. Wang, and Y. Zhou. 2009. Purification of anatid herpesvirus 1 particles by tangential-flow ultrafiltration and sucrose gradient ultracentrifugation. J. Virol. Methods 161:1–6.

He, T., M. Wang, A. Cheng, Q. Yang, R. Jia, Y. Wu, J. Huang, S. Chen, X.-X. Zhao, and M. Liu. 2020. Duck enteritis virus pUL47, as a late structural protein localized in the nucleus, mainly depends on residues 40 to 50 and 768 to 777 and inhibits IFN-β signalling by interacting with STAT1. Vet. Res. 51:1–12.

Hu, X., M. Wang, S. Chen, R. Jia, D. Zhu, M. Liu, Q. Yang, K. Sun, X. Chen, and A. Cheng. 2017. The duck enteritis virus early protein, UL13, found in both nucleus and cytoplasm, influences viral replication in cell culture. Poult. Sci. 96:2899–2907.

Johnson, D. C., and J. D. Baines. 2011. Herpesviruses remodel host membranes for virus egress. Nat. Rev. Microbiol. 9:382–394.

Kato, A., J. Arii, I. Shiratori, H. Akashi, H. Arase, and Y. Kawaguchi. 2009. Herpes simplex virus 1 protein kinase Us3 phosphorylates viral envelope glycoprotein B and regulates its expression on the cell surface. J. Virol. 83:250–261.

Kato, A., Z. Liu, A. Minowa, T. Imai, M. Tanaka, K. Sugimoto, Y. Nishiyama, J. Arii, and Y. Kawaguchi. 2011. Herpes simplex virus 1 protein kinase Us3 and major tegument protein UL47

reciprocally regulate their subcellular localization in infected cells. J. Virol. 85:9599–9613.

Kato, A., M. Yamamoto, T. Ohno, M. Tanaka, T. Sata, Y. Nishiyama, and Y. Kawaguchi. 2006. Herpes simplex virus 1-encoded protein kinase UL13 phosphorylates viral Us3 protein kinase and regulates nuclear localization of viral envelopment factors UL34 and UL31. J. Virol. 80:1476–1486.

Klupp, B. G., T. Hellberg, H. Granzow, K. Franzke, B. Dominguez Gonzalez, R. E. Goodchild, and T. C. Mettenleiter. 2017. Integrity of the linker of nucleoskeleton and cytoskeleton is required for efficient herpesvirus nuclear egress. J. Virol. 91:e00330 -00317.

Malhas, A., C. Goulbourne, and D. J. Vaux. 2011. The nucleoplasmic reticulum: form and function. Trends Cell Biol. 21:362–373.

Mettenleiter, T. C., F. Müller, H. Granzow, and B. G. Klupp. 2013. The way out: what we know and do not know about herpesvirus nuclear egress. Cell. Microbiol. 15:170–178.

Mou, F., T. Forest, and J. D. Baines. 2007. US3 of herpes simplex virus type 1 encodes a promiscuous protein kinase that phosphorylates and alters localization of lamin A/C in infected cells. J. Virol. 81:6459–6470.

Mou, F., E. Wills, and J. D. Baines. 2009. Phosphorylation of the UL31 protein of herpes simplex virus 1 by the US3-encoded kinase regulates localization of the nuclear envelopment complex and egress of nucleocapsids. J. Virol. 83:5181–5191.

Mou, F., E. G. Wills, R. Park, and J. D. Baines. 2008. Effects of lamin A/C, lamin B1, and viral US3 kinase activity on viral infectivity, virion egress, and the targeting of herpes simplex virus UL34-encoded protein to the inner nuclear membrane. J. Virol. 82:8094–8104.

Proft, A., B. Spiesschaert, S. Izume, S. Taferner, M. J. Lehmann, and W. Azab. 2016. The role of the equine herpesvirus type 1 (EHV-1) US3-encoded protein kinase in actin reorganization and nuclear egress. Viruses 8:275.

Reynolds, A. E., B. J. Ryckman, J. D. Baines, Y. Zhou, L. Liang, and R. J. Roller. 2001. UL31 and UL34 proteins of herpes simplex virus type 1 form a complex that accumulates at the nuclear rim and is required for envelopment of nucleocapsids. J. Virol. 75:8803–8817.

Reynolds, A. E., E. G. Wills, R. J. Roller, B. J. Ryckman, and J. D. Baines. 2002. Ultrastructural localization of the herpes simplex virus type 1 UL31, UL34, and US3 proteins suggests specific roles in primary envelopment and egress of nucleocapsids. J. Virol. 76:8939–8952.

Ryckman, B. J., and R. J. Roller. 2004. Herpes simplex virus type 1 primary envelopment: UL34 protein modification and the US3-UL34 catalytic relationship. J. Virol. 78:399–412.

Schumacher, D., C. McKinney, B. B. Kaufer, and N. Osterrieder. 2008. Enzymatically inactive US3 protein kinase of Marek's disease virus (MDV) is capable of depolymerizing F-actin but results in accumulation of virions in perinuclear invaginations and reduced virus growth. Virology 375:37–47.

Shibazaki, M., A. Kato, K. Takeshima, J. Ito, M. Suganami, N. Koyanagi, Y. Maruzuru, K. Sato, and Y. Kawaguchi. 2020. Phosphoregulation of a conserved herpesvirus tegument protein by a virally encoded protein kinase in viral pathogenicity and potential linkage between its evolution and viral phylogeny. J. Virol. 94:e01055 -01020.

Van den Broeke, C., M. Radu, M. Deruelle, H. Nauwynck, C. Hofmann, Z. M. Jaffer, J. Chernoff, and H. W. Favoreel. 2009. Alphaherpesvirus US3-mediated reorganization of the actin cytoskeleton is mediated by group A p21-activated kinases. Proc. Natl. Acad. Sci. 106:8707–8712.

Wisner, T. W., C. C. Wright, A. Kato, Y. Kawaguchi, F. Mou, J. D. Baines, R. J. Roller, and D. C. Johnson. 2009. Herpesvirus gB-induced fusion between the virion envelope and outer nuclear membrane during virus egress is regulated by the viral US3 kinase. J. Virol. 83:3115–3126.

Wu, Y. 2015. Genome Analysis of Duck Plague Virus Chinese Virulent Strain and Preliminary Study of UL55 Gene Fuction. Sichuan Agricultural University, Sichuan.

You, Y., A.-C. Cheng, M.-S. Wang, R.-Y. Jia, K.-F. Sun, Q. Yang, Y. Wu, D. Zhu, S. Chen, and M.-F. Liu. 2017. The suppression of apoptosis by α-herpesvirus. Cell Death. Dis. 8:e2749−e2749.

You, Y., T. Liu, M. Wang, A. Cheng, R. Jia, Q. Yang, Y. Wu, D. Zhu, S. Chen, and M. Liu. 2018. Duck plague virus Glycoprotein J is functional but slightly impaired in viral replication and cell-to-cell spread. Sci. Rep. 8:1–9.

Yuan, G.-P., A.-C. Cheng, M.-S. Wang, F. Liu, X.-Y. Han, Y.-H. Liao, and C. Xu. 2005. Electron microscopic studies of the morphogenesis of duck enteritis virus. Avian Dis. 49:50–55.